King Saud University

Arabian Journal of Chemistry

www.ksu.edu.sa
www.sciencedirect.com

ORIGINAL ARTICLE

Bio-guided chemical characterization and nano-formulation studies of selected edible volatile oils with potential antibacterial and anti-SARS-CoV-2 activities

Mohamed S. Refaey [a,*,1], Marwa A. A. Fayed [a,1], Omnia Kutkat [b], Yassmin Moatasim [b], Nahla Sameh Tolba [c], Anis Anis [d], Ahmed M. Elshorbagy [a], Khloud Nassar [e], Khaled A. M. Abouzid [f], Yaseen A. M. M. Elshaier [g], Mohamed F. El-Badawy [h]

[a] Department of Pharmacognosy, Faculty of Pharmacy, University of Sadat City, Menoufia 32897, Egypt
[b] Center of Scientific Excellence for Influenza Viruses, National Research Centre (NRC), Giza 12622, Egypt
[c] Department of Pharmaceutics, Faculty of Pharmacy, University of Sadat City, Menoufia 32897, Egypt
[d] Department of Pathology, faculty of Veterinary Medicine, University of Sadat City, Egypt
[e] Department of biochemistry, Faculty of Pharmacy, University of Sadat City, Menoufia 32897, Egypt
[f] Pharmaceutical Chemistry Department, Faculty of Pharmacy, Ain Shams University, Abbassia 11566, Cairo, Egypt
[g] Department of Organic and Medicinal Chemistry, Faculty of Pharmacy, University of Sadat City, Menoufia 32897, Egypt
[h] Microbiology and immunology Department, Faculty of Pharmacy, University of Sadat City, Menoufia 32897, Egypt

Abstract The recent pandemic caused by severe acute respiratory syndrome coronavirus 2 (SARS-CoV-2) has opened the door to potential threats of the respiratory system. The discovery of drugs from natural sources is one of the most important strategies for treating the upper respiratory tract. In this study, we investigated the selected formulated EOs activities against Gram-negative *(E. coli, K. pneumonia,* and *P. aeruginosa)* and Gram-positive *(S. aureus, E. fecalis)* bacteria and against the SARS-CoV-2 virus, with the mode of action investigated as anti-SARS-CoV-2. *Cinnamomum zeylanicum* and *Syzygium aromaticum* EOs were the most promising antibacterial oils. *C. zeylanicum*

Production and hosting by Elsevier

EO showed MIC values of 1, 1, 2, ≤0.5, and 8 µg/mL against *E. coli, K. pneumoniae, P. aeruginosa, S. aureus,* and *E. fecalis*, respectively, while *S. aromaticum* EO showed MIC values of 8, 4, 32, 8, 32 µg/mL against the same organisms. The cytotoxic activity of the oil samples was tested in VERO-E6 cells using (MTT) assay and showed that the safest oil was *F. vulgare*, then *L. nobilis, C. carvi, S. aromaticum,* and *E. globulus*. The most potent antiviral EOs were *C. zeylanicum* oil and *S. aromaticum*, with IC_{50} value of 15.16 and 96.5 µg/mL, respectively. Moreover, the safety index of *S. aromaticum* EO (26.3) was greater than the oil of *C. zeylanicum* (7.25). The mechanism by which *C. zeylanicum* oil exerts its antiviral activity may involve both the virucidal effect and its impact on viral reproduction. The nano-emulsion dosage form of the potent EOs was prepared and re-examined against the same bacterial and viral strains. Finally, the chemical characterization of these promising essential oils was analyzed and identified using the GC–MS approach. To the best of our knowledge, this is the first report concerning the *in vitro* investigation of anti-SARS-CoV-2 activity of these selected essential oils, along with a proposed mechanism for the potent oil's activity.

1. Introduction

Infection of the respiratory tract is one of the commonest illnesses in the general population, resulting in severe morbidity (June 2015, Ács et al., 2018). Pneumonia accounted for 13% of the deaths of post-neonatal infants (1–59 months) in 2012 (Ács et al., 2018). Respiratory tract infections, which are the primary reason for clinic visits and antibiotic prescriptions, account for over 50 million deaths worldwide (El-Kased 2016). The infections of the upper and lower respiratory tracts are caused by several bacteria. Clinical isolates of *Staphylococcus aureus* have shown resistance to last-resort medications, such as linezolid and vancomycin, which is making the resistance issue worse (Karami et al., 2021). Besides, certain viral infections of the respiratory tract have been linked to disease pandemics, such as the Middle East respiratory syndrome coronavirus (MERS-CoV), influenza, and more recently the novel severe acute respiratory syndrome coronavirus 2 (SARS-CoV-2) infection-causing COVID-19 disease that is currently sweeping the globe**.** As of January 22, 2022, about 346 million COVID-19 cases had been documented worldwide resulting in 5.59 million fatalities. These demonstrate the profoundly detrimental effects of respiratory diseases on people's personal life, societal advancement, and existence (Molinari 2009, Oriola and Oyedeji 2022). The upper respiratory tract (URT) is the entry point for SARS-CoV-2, and SARS-CoV-2 most likely interacts with the URT microbiome and will progress to severe diseases with the emergence of secondary bacterial infections. The most common respiratory symptoms in patients with COVID-19 sequelae are a persistent cough (mostly dry) and shortness of breath, while dyspnea is the most common persistent symptom after COVID-19 recovery (Nguyen-Ho et al., 2022). To address these issues, novel medications must be created that treat both acute and chronic respiratory conditions more safely and effectively. Several attempts have been made to develop coronaviral inhibitors as high-throughput screening of structurally varied compound libraries (Zhu et al., 2020), structure-based drug design (Zhang et al., 2020), in silico examinations (Zaidman et al., 2021, Unoh et al., 2022), and drug repurposing (Silva et al., 2021, Abdelhady et al., 2022). Despite significant efforts, the US Food and Drug Administration (FDA) has only licensed a few drugs for the treatment of mild-to-moderate coronavirus disease. One of the potential remedies to this global issue is the study of the antibacterial and antiviral properties of essential oils (EOs), which are widely utilized today in the food, cosmetic, and healthcare industries. Additionally, because of their efficacy against bacteria and inflammation, they provide an efficient remedy for the treatment of respiratory tract infections (Horváth and Ács 2015). EOs are extremely fascinating natural compounds that have a variety of biological characteristics. Thyme and clove oils, which have a high phenol concentration, have antibacterial qualities. They can be employed as important materials in the treatment of many respiratory tract disorders because of their extensive and complex actions, such as an antibacterial, antiviral, anti-inflammatory, mucolytic, bronchodilator, etc. (Horváth and Ács 2015). Numerous different chemical compounds, primarily mono- and sesquiterpenoids and phenylpropanoids, may be found in essential oil (Refaey et al., 2022). They are given therapeutically through inhalation (eucalyptus oil, for example), oral administration (peppermint oil), and transdermal application (e.g., rosemary oil) (Horváth and Ács 2015). Some EOs are only utilized in applications based on long-term usage, whereas others can be used in applications based on well-established use (Horváth and Ács 2015). The antibacterial and antiviral properties of the essential oils isolated from several plants, including fennel, anise, peppermint, thyme, and tea tree, have been documented for the treatment of respiratory tract disorders such as *Stenotrophomonas maltophilia*, parainfluenza, and *Haemophilus influenza* (Horváth and Ács 2015, Balázs et al., 2019). Nanoparticles are recognized as the standard of contemporary pharmacological treatment since they consistently offer fresh leads with unique biological mechanisms of action against developing illnesses (Ács et al., 2018). The importance of nanoparticles in the creation of novel drugs is highlighted by the fact that 60% of medications now on the market are made from natural ingredients (Molinari 2009). In general, using oil in water nano-emulsions (NEs) has considerable promise for displacing conventionally emulsified oil. The biological efficacy can be improved, and the dosage of the active component can be decreased when utilizing oil in water NEs (Campolo et al., 2020).

This work aims to discover an edible volatile oil with a multi-pharmacological effect (anti-SARS-CoV-2 and antibacterial) capable of reducing oral viral load in infected people and decreasing the risk of viral transmission. In this study, we have selected eight medicinal plants based on their availability from both commercial and cultivated sources. The traditional uses and biological activities of these plants were summarized in (Table S1). The selected oils were examined for their potential antibacterial, cytotoxic, and antiviral activities against different bacterial pathogens as well as against SARS-CoV-2. The oil with potential activity will be formulated as NE and will be re-examined against the same microbial and viral strains. The composition of the potent essential oils will be examined utilizing GC–MS analysis.

2. Material and methods

2.1. Plant material

Five plants in this work, *Origanum majorana* herb*, Syzygium aromaticum* flower buds*, Carum carvi* fruits*, Cinnamomum zeylanicum* bark, and *Laurus nobilis* leaves, were purchased from

the herbal commercial market in September 2021, Cairo, Egypt, while *Pelargonium graveolens, Foeniculum vulgare, and Eucalyptus globulus* leaves were collected from the Experimental Plants Station, Cairo University, Cairo, Egypt (30.0274° N, 31.2091° E). The plants were identified and authenticated by Dr. Mohamed F. Azzazy, professor of plant ecology at the Surveys of Natural Resources Department, Environmental Studies and Research Institute, University of Sadat City, Egypt. The voucher specimens were deposited in the herbarium of Environmental Studies and Research Institute, Sadat City, Egypt.

2.2. Extraction of essential oil

The plant parts used in this study were pulverized into a weight (250 g) in a blender (Braun, Kronbergim Taunus, Germany) and hydro-distilled using Clevenger-type equipment under atmospheric pressure and at a boiling temperature of roughly 100 °C) for three hours (Refaey et al., 2022). The essential oils were distilled, then they were gathered and dried over anhydrous sodium sulfate (Lanxess, Thane, India). The oil samples were stored in opaque glass vials at a freezing (4 °C) temperature until further investigation. The following formula was used to determine the essential oil yields.

The yield of essential oil = weight of essential oil (g) / weight of sample (g) × 100.

2.3. Gas chromatography-mass spectrometry analysis (GC–MS)

The GC–MS system (Agilent Technologies) was equipped with a gas chromatograph (7890B) and mass spectrometer detector (5977A) at the Central Laboratories Network, National Research Centre, Cairo, Egypt. Samples were diluted with hexane (1:19, v/v). The GC was equipped with a DB-WAX column (30 m × 250 μm internal diameter and 0.25 μm film thickness, Thermo Scientific, Austin, TX, USA). Analyses were carried out using hydrogen as the carrier gas at a flow rate of 3.0 mL/min at a split lower volume of 1 μl and the following temperature program: 40 °C for 2 min; rising at 7 °C / min to 250 °C and held for 8 min. The injector and detector were held at 250 °C and 250 °C, respectively. Mass spectra were obtained by electron ionization (EI) at 70 eV; using a spectral range of m/z 40–550 and solvent delay of 3.5 min. Identification of different constituents was determined by comparing the spectrum fragmentation pattern with those stored in Wiley and NIST mass spectral library data.

2.4. Synthesis of essential oil nano-emulsion

2.4.1. Synthesis of C. zeylanicum oil nano-emulsion

A 6% of *C. zeylanicum* oil NE was prepared using a magnetic stir plate for 30 min at a constant speed (700 rpm). 44.5 mL of sterile distilled water, 2.5 mL of Tween 80, and 3 mL of *C. zeylanicum* oil were mixed and stirred. Ultrasonicator (model UP400S, power maximum 400 W, Dr. Hielscher GmbH, Germany) was used to produce NE. The amplitude was set to 60. The wattages used were in the range of 50 –70. The experiment was done in an ice bath to avoid heating, and the sonication time was 20 min. (Paudel et al., 2019).

2.4.2. Synthesis of S. aromaticum oil nano-emulsion

To obtain oil in water emulsions (O/W) at ambient temperature, the designated amounts of *S. aromaticum* oil (10% v/v), water up to 100% v/v), and a mixture of (5 % w/v) surfactants (Span_ 80/Tween_ 80) were blended. The samples were prepared by ultrasound method. Emulsification by sonication was prepared using an ultrasonic processor (model UP400S, power maximum = 400 W, Dr. Hielscher GmbH, Germany). This ultrasonic transducer converts applied electrical waves into ultrasonic waves. In addition, the converter vibrated and transmitted at a constant frequency (24 kHz) for 15 mins in an ice bath.

A frequently used method for the selection of surfactants as emulsifying agents is known as the hydrophilic-lipophilic balance (HLB) method. The HLB number of the mixed surfactant system was calculated by the following equation:

$$HLB\ desired = (\%\ surfactant\ A) \times (HLB\ Surfactant\ A) \\ + (\%\ surfactant\ B) \times (HLB\ Surfactant\ B)$$

(1)

Tween 80 with an HLB value of 15.0 and Span 80 with an HLB value of 4.3, were selected for the preparation of NEs. The value HLB of 9 (Span 80 = 56% and Tween 80 = 44%) was defined based on Eq. (1) with the concentration of mixed surfactants in an emulsion system (Shahavi et al., 2019).

2.5. Characterization of the prepared nano-emulsion

2.5.1. Size and zeta potential

2.5.1.1. Particle size and polydispersity index (PDI) determination. Particle size analysis (mean size and polydispersity index (PDI)) of the prepared essential oil NE was performed using dynamic light scattering after appropriate dilution with distilled water. (Zetasizer, Nanoseries, Nano-zs; Malvern Instruments, Malvern, Worcestershire, UK). At room temperature, 30 μl of the NE was diluted with 3 mL of 25 °C water. Particle size data were expressed as the mean of the Z-average of three independent batches of the NEs. All measurements were carried out in triplicates, and the mean values, as well as SD, were calculated.

2.5.1.2. Zeta potential measurement. Charges on the prepared essential oils NE were investigated, as well as the values of their zeta potential, were obtained using a Zeta-sizer under standard operation conditions after appropriate dilution of the samples with distilled water.

Each experiment was done in triplicates, and results were expressed as mean values ± SD.

2.5.1.3. Size and shape. A 200-mesh copper specimen grid coated with film was used to hold 20 Âμl of diluted samples for 10 min before the extra liquid was filtered out with filter paper. Next, one drop of 3% phosphotungstic acid was used to stain the grid, and it was given three minutes to dry. After drying, the coated grid was examined with a TEM microscope (JEOL JEM-2100 high-resolution transmission electron microscope). The samples were evaluated using an accelerating voltage of 200 kV, respectively.

2.6. Antibacterial activity

2.6.1. Determination of antimicrobial susceptibility testing (AST)

Antimicrobial susceptibility testing was primarily done for the tested oils by the modified Kirby-Bauer method using sterile discs loaded with 5 µl of the crude essential oils. Also, AST was determined by the broth microdilution method to determine the MIC values.

2.6.2. Modified Kirby-Bauer method (disc diffusion)

A sterile cotton swab was dipped into the bacterial suspension (adjusted to 0.5 McFarland) of the tested bacterial or fungal strains and the excess suspension was removed by pressing the cotton swab against the wall of the tube containing the microbial suspension. The swab was streaked all over the surface of the Muller-Hinton agar (MHA) plate three times by rotating the plate at an angle of 60° after each application. Finally, the swab was passed around the edge of the agar surface. The inoculated MHA plates were left to dry for a few minutes at room temperature with the lid closed. The loaded discs with tested oils were placed on the inoculated plates using sterile forceps. Each disc was gently pressed down to ensure even contact with the medium. The plates were then incubated overnight at 37 °C. On the next day, the diameter of the inhibition zone (including the diameter of the discs) was measured with a ruler under the surface of the plate, and the results were recorded in mm (Vandepitte et al., 2003).

2.6.3. Broth microdilution method

The broth microdilution method was performed in 96-well microtiter plates using different concentrations of the investigated essential oils. All columns of the sterile 96-well plate was filled with 100 µl of sterile distilled water (SDW), except column No. 1 which was filled with 159 µl of sterile distilled water, to which 41 µl of the tested extract was added to obtain a final concentration of 1024 µg / 200 µl after addition of the broth containing the tested organism. The last two rows of 96-well plates were used only as positive and negative controls, respectively.

Hundred µl from the tested extract stock solutions in column No. 1 were withdrawn and added to the next wells (containing 100 µl of SDW) in column No. 2 and mixed by pipetting 3–6 times, then 100 µl from the next wells were withdrawn and added to the third wells in column No. 3 and mixed well by pipetting 3–6 times. This process was repeated until reaching well No.12 in which the last 100 µl withdrawn from well No. 12 were discarded. After serial dilution of the tested essential oils was done, all wells of the plate were filled with 100 µl of 5,5′-dithiobis succinimidyl-2-nitrobenzoate (DSNB), containing the tested isolate, and mixed well by pipetting 3–6 times. The plates were **incubated** at 37 °C for 18 h (Schwalbe 2007).

2.6.4. Preparation of the first concentration for further twofold dilution

The first desired concentration was achieved by the following equation: $C_1V_1 = C_2V_2$, where C_1 represents the originally tested extract stock concentration, V_1 represents the volume required from the original stock concentration to obtain the desired concentration, C_2 represents the desired concentration, and V_2 represents the volume containing the desired concentration. For example, when the first desired concentration is 1024 µg / 200 µl, the equation will be as follows; 10000 µg × V_1 = 1024 × 200 µl, so the desired volume was 20.48 µl, this volume was doubled to overcome the dilution in the first well by DSNB, so 40.96 µl from the antibiotic stock solution was completed to 200 µl by adding approximately 159 µl of SDW.

2.6.5. Inoculum preparation (direct colony suspension method)

The direct colony suspension method was performed by suspending a few colonies of the tested isolate in sterile normal saline. The prepared suspension was adjusted to achieve turbidity equivalent to 0.5 McFarland standard, which is approximately equivalent 1to 2×10^8 CFU/mL, which was further diluted to obtain a final inoculum concentration of 5×10^5 CFU/mL in each well of a microtiter plate. This was done by adding 35 µl of the 0.5 McFarland adjusted inoculum to 35 mL of double strength nutrient broth (DSNB). The inoculated broth was used directly within 15 min of preparation (Wikler 2006).

2.7. Cytotoxicity assay on cells

2.7.1. In vitro MTT cytotoxicity assay

Studies of cell toxicity almost universally use the *in vitro* MTT cytotoxicity test to measure the safe concentration of each oil on the cells (Ghasemi et al., 2021). To assess the half maximal cytotoxic concentration (CC_{50}), for the determination of safety index (SI), stock solutions of the test oils were prepared in 10 % dimethyl sulfoxide (DMSO, Serva, Germany) in ddH$_2$O and diluted further to the working solutions with Dulbecco's modified eagle medium (DMEM, Lonza, Walkersville.MD, USA). The cytotoxic activity of the oils and nano-formulated samples was tested in VERO-E6 cells by using the 3-(4, 5-dimethylthiazol-2-yl)-2, 5-diphenyltetrazolium bromide (MTT) method with minor modifications (Denizot and Lang 1986, Ghanbari et al., 2022). Briefly, the cells were seeded in 96 well plates (Greiner Bio-One, Germany) with growth medium (100 µl/well at a density of 3×10^5 cells/mL) and incubated for 24 h in humidified cell culture incubator (37 °C in 5% CO$_2$, Thermo Fisher Scientific). After 24 h, cells were washed three times with 1x PBS treated with various concentrations of the tested oils in triplicates. 24 h later, the supernatant was discarded, and cell monolayers were washed with sterile 1x phosphate buffer saline (PBS) 3 times, and MTT solution (20 µl of 5 mg/mL stock solution) was added to each well and incubated at 37 °C for 4 h followed by medium aspiration. In each well, the formed formazan crystals were dissolved with 200 µl of DMSO. The absorbance of formazan solutions was measured at λ_{max} 540 nm with 620 nm as a reference wavelength using a multi-well plate reader (Anthos Zenyth 200rt Microplate Reader). The percentage of cytotoxicity compared to the untreated cells was determined with the following equation.

The plot of % cytotoxicity versus sample concentration was used to calculate the concentration that exhibited 50 % cytotoxicity (CC_{50}).

2.8. Antiviral activity

2.8.1. Inhibitory concentration 50% (IC_{50}) anti SARS-CoV-2:

Inhibitory concentration 50% (IC_{50}) to determine the concentrations that inhibit 50% of the propagated virus. In 96-well

tissue culture plates, 2.4×10^4 Vero-E6 cells were distributed in each well and incubated overnight at 37 °C in a humidified incubator under 5% CO_2 conditions. The cell monolayers were then washed once with 1x PBS and subjected to virus adsorption (hCoV-19/Egypt/NRC-03/2020 (Accession Number on GSAID: EPI_ISL_430820)) for 1 h at room temperature (RT). The cell monolayers were further overlaid with 100 μl of DMEM containing varying concentrations of the test compounds. Following incubation at 37 °C in a 5% CO_2 incubator for 72 h, the cells were fixed with 100 μl of 4% paraformaldehyde for 2 h and stained with 0.1% crystal violet in distilled water for 15 min at RT. The crystal violet dye was then dissolved using 100 μl absolute methanol per well, and the optical density of the color was measured at 570 nm using an Anthos Zenyth 200rt plate reader (Anthos Labtec Instruments, Heerhugowaard, Netherlands). The IC_{50} of the compound is required to reduce the virus-induced cytopathic effect (CPE) by 50%, relative to virus control, and it is important for calculating the Safety Index (SI) = CC_{50}/IC_{50}.

2.9. Mode of action for virus inhibition

The possible mode of action of the potent selected essential oil against virus inhibition was examined at three different stages of the virus propagation cycle and based on three main possible modes of action: (i) inhibition of budding and viral replication, (ii) the ability of the oil to inhibit the attachment of the virus to infected cells through membrane fusion, which is known as blocking the viral entry (viral adsorption), and (iii) the direct effect of the oil to inactivate the virus's viability (virucidal activity). Additionally, the above-mentioned mode of action could account for the recorded antiviral activities either independently, or in combinations.

2.9.1. Viral replication

The viral replication assay was applied according to Kuo Y. et al (Kuo et al., 2002).

2.9.2. Viral adsorption

The viral adsorption assay was performed according to Zhang L. et al (Zhang et al., 2020).

2.9.3. Virucidal mode

The virucidal assay was carried out according to Schuhmacher A. et al (Schuhmacher et al., 2003).

2.10. Ethical approval

The study was approved by the ethics committee of NRC (approval number: NRC-20074), and all procedures and experiments were carried out in accordance with the approved protocol.

3. Results and discussion

The hydro-distillation of *O. majorana* herb, *S. aromaticum* flower buds, *C. carvi* fruits, *C. zeylanicum* bark, *L. nobilis* leaves, *P. graveolens* leaves, *F. vulgare* fruits, and *E. globulus* leaves led to the isolation of clear essential oil residues with a fragrant odor with a yield of 3.69 %, 7.53 %, 0.22 %, 0.33 %, 0.35 %, 2.52 %, 0.97 %, and 0.12 % (w/w), respectively.

3.1. Antimicrobial susceptibility testing of pure oils

The result of susceptibility testing of the total essential oils obtained from the eight plants included in the current work (Table 1) revealed that the oil extract of *C. zeylanicum* was the most effective one against the tested Gram-positive and Gram-negative bacteria, in which the MIC of *C. zeylanicum* volatile oils was ≤ 0.5 and 8 μg/mL for *S. aureus* and *E. fecalis*, respectively, and 1 μg/mL for *E. coli* and *K. pneumoniae*. In this context, *C. zeylanicum* volatile oil was the only oil that had activity against *P. aeruginosa*.

The present study also exhibited that the volatile oil of *S. aromaticum* ranked as the 2nd most effective agent against Gram-negative and Gram-positive bacteria where the MIC values for *E. coli* and *K. pneumoniae* were 4 and 8 μg/mL, respectively, and 8 and 32 μg/mL for *S. aureus* and *E. fecalis*, respectively (Table 1).

In contrast to the reported activity of volatile oils extracted from *C. zeylanicum* and *S. aromaticum* against Gram-positive and Gram-negative bacteria, the volatile oil of *F. vulgare* showed no activity against any tested bacteria.

As regards the other tested volatile oils, the current work revealed that the volatile oils of *E. globulus* and *C. carvi* have the same activity against Gram-negative bacteria represented by *E. coli* and *K. pneumoniae* in which the MIC values were 16 and 8 μg/mL, respectively. On the other hand, the volatile oil *E. globulus* was superior to *C. carvi* against Gram-positive bacteria, as shown in (Table 1).

3.2. Antimicrobial susceptibility testing of nano-emulsion formulated oils

The current study revealed that the formulated NE of *C. zeylanicum* essential oil was found to enhance the antibacterial activity by decreasing the MIC value by at least two-folds, in which the MIC value of *C. zeylanicum* NE against *E. coli* and *K. pneumoniae* was decreased from 1 μg/mL for each to ≤ 0.5 for each. Similar results were seen for Gram-positive bacteria, where *S. aureus* and *E. fecalis'* MIC values were dropped from 8 and 32 μg/mL to 0.125 and 2 μg/mL, respectively (Table 2).

As regards the essential oil of *S. aromaticum*, the present study showed that, the NE formulation potentiated the antibacterial activity by decreasing the MIC value against *E. coli* and *K. pneumoniae* from 4 and 8 μg/mL to 2 and 4 μg/mL, respectively. It was also found that the NE form of *S. aromaticum* essential oil decreased the MIC values of *S. aureus* and *E. fecalis* from 8 and 32 μg/mL to 2 and 8 μg/mL, respectively. In terms of *P. aeruginosa* MIC value, the NE formulation increased the antipseudomonal activity of *C. zeylanicum* and *S. aromaticum* by decreasing the MIC value by two and four folds, respectively.

3.3. Cytotoxicity assay

The results of cytotoxicity (Fig. 1) showed that the safest oil was *F. vulgare* oil with a CC_{50} = 4922 μg/mL followed by

Table 1 The MIC of pure non-formulated essential oil against different bacterial strains.

| Plant used | Minimum Inhibitory Concentration (MIC) µg/mL | | | | |
| | Gram-negative strains | | | Gram-positive strains | |
	E. coli ATCC 22,925	K. pneumonia ATCC 700,603	P. aeruginosa ATCC 27,853	S. aureus ATCC 29,213	E. fecalis ATCC 29,212
Pelargonium graveolens	8	32	> 1024	8	512
Origanum majorana	32	32	> 1024	8	512
Syzygium aromaticum	4	8	32	8	32
Foeniculum vulgare	> 1024	> 1024	> 1024	> 1024	> 1024
Carum carvi	16	8	> 1024	32	> 1024
Cinnamomum zeylanicum	1	1	2	≤ 0.5	8
Eucalyptus globulus	16	8	256	2	128
Laurus nobilis	64	64	256	16	> 1024
Gentamicin	0.5	–	1	0.5	4–16
Tetracycline	0.5	–	8	0.5	8
Vancomycin	NA	–	NA	0.5	1
Oxacillin	NA	–	NA	0.5	8
Fosfomycin	0.5	–	2	2	32
Linezolid	NA	–	NA	1	1

Table 2 The MIC of nanoemulsion formulated *C. zeylanicum nano* and *S. aromaticum* against different bacterial strains.

| Plant used | Minimum Inhibitory Concentration (MIC) µg/mL | | | | |
| | Gram-negative strains | | | Gram-positive strains | |
	E. coli ATCC 22,925	K. pneumonia ATCC 700,603	P. aeruginosa ATCC 27,853	S. aureus ATCC 29,213	E. fecalis ATCC 29,212
Nano-emulsion Control	> 1024	> 1024	> 1024	> 1024	> 1024
C. zeylanicum nanoemulsion	≤ 0.5	≤ 0.5	≤ 0.5	0.125	2
S. aromaticum nanoemulsion	2	4	2	2	8

L. nobilis, *C. carvi*, *S. aromaticum,* and *Eucalyptus globulus* with CC_{50s} = 2888, 2637, 2542, and 2533 µg/mL, respectively.

3.4. Antiviral activity

3.4.1. Inhibitory concentration 50 (IC50) anti SARS-CoV-2
Inhibitory concentration (IC_{50}) (Fig. 1) is important for determining the concentration of oil that inhibits viral propagation by half; the most potent one with antiviral activity was *C. zeylanicum* oil; it had an IC_{50} of 15.16 µg/mL but a low CC_{50}, so the safety index (CC_{50}/IC_{50}) was 110.6/15.16 = 7.25. On the other hand, *S. aromaticum* oil had less antiviral activity than *C. zeylanicum* oil, with an IC_{50} of 96.5 µg/mL, but a high CC_{50} of 2542 µg/mL, so the safety index was 2542/96.5 = 26.3. The most potent oils were *C. zeylanicum* oil and *S. aromaticum* oil, so they were formulated in oil NE. The non-nanoemulsion form of the oil was found to be more active against the virus than the nano form, with an IC_{50} of 778.3 g/mL for *S. aromaticum* oil in NE form and 302.5 g/mL for *C. zeylanicum* oil in NE form (Fig. 2).

3.5. Mode of action

This assay was established to determine the mode of action for *C. zeylanicum* oil, which had an IC_{50} of 15.16 µg/mL. The results showed that this oil affects viral propagation by two mechanisms: virucidal effect and replication, after using different concentrations as shown in Fig. 3.

3.6. Size and zeta potential

3.6.1. Particle size and polydispersity index (PDI) determination
The performance of NE depends heavily on the droplet diameter and droplet size distribution. Light scattering methods, as well as scanning or transmission electron microscopy, can be used to determine the droplet diameter and droplet size distribution. If a small droplet size distribution emulsion cannot be created, then the formulation of NE with a narrow size distribution will be a challenge (Tadros et al., 2004). The *C. zeylanicum* NE formulation had a high polydispersity index (PDI) in
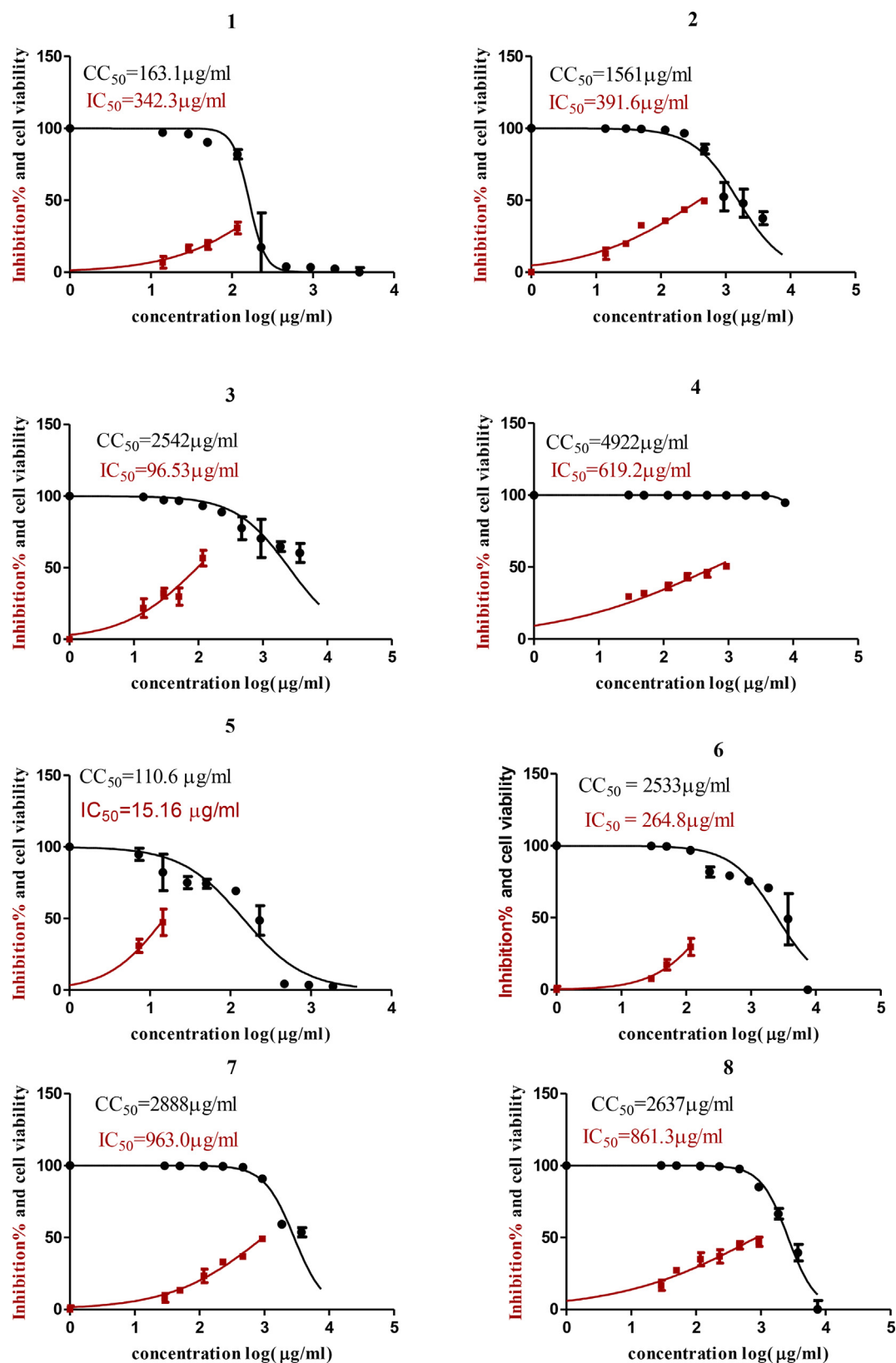
Fig. 1 Graph of Cytotoxicity concentration 50 % (CC$_{50}$) and anti SARS-CoV-2 inhibitory concentration 50% (IC$_{50}$) of (1) *P. graveolens*; (2) *O. majorana*; (3) *S. aromaticum*; (4) *Foeniculum vulgare*; (5) *C. zeylanicum*; (6) *E. globulus*; (7) *L. nobilis* and (8) *C. carvi*. Cytotoxicity concentration 50 % (CC$_{50}$) and Inhibitory concentration 50% (IC$_{50}$) values were calculated using nonlinear regression analysis of GraphPad Prism software (version 5.01) by plotting log inhibitor versus normalized response (variable slope).

Fig. 2 Graph of Cytotoxicity concentration 50% (CC$_{50}$) and anti SARS-CoV-2 inhibitory concentration 50% (IC$_{50}$) of (3) *S. aromaticum* and (5) *C. zeylanicum* oils NEs. Cytotoxicity concentration 50 % (CC$_{50}$) and Inhibitory concentration 50% (IC$_{50}$) values were calculated using nonlinear regression analysis of GraphPad Prism software (version 5.01) by plotting log inhibitor versus normalized response (variable slope).
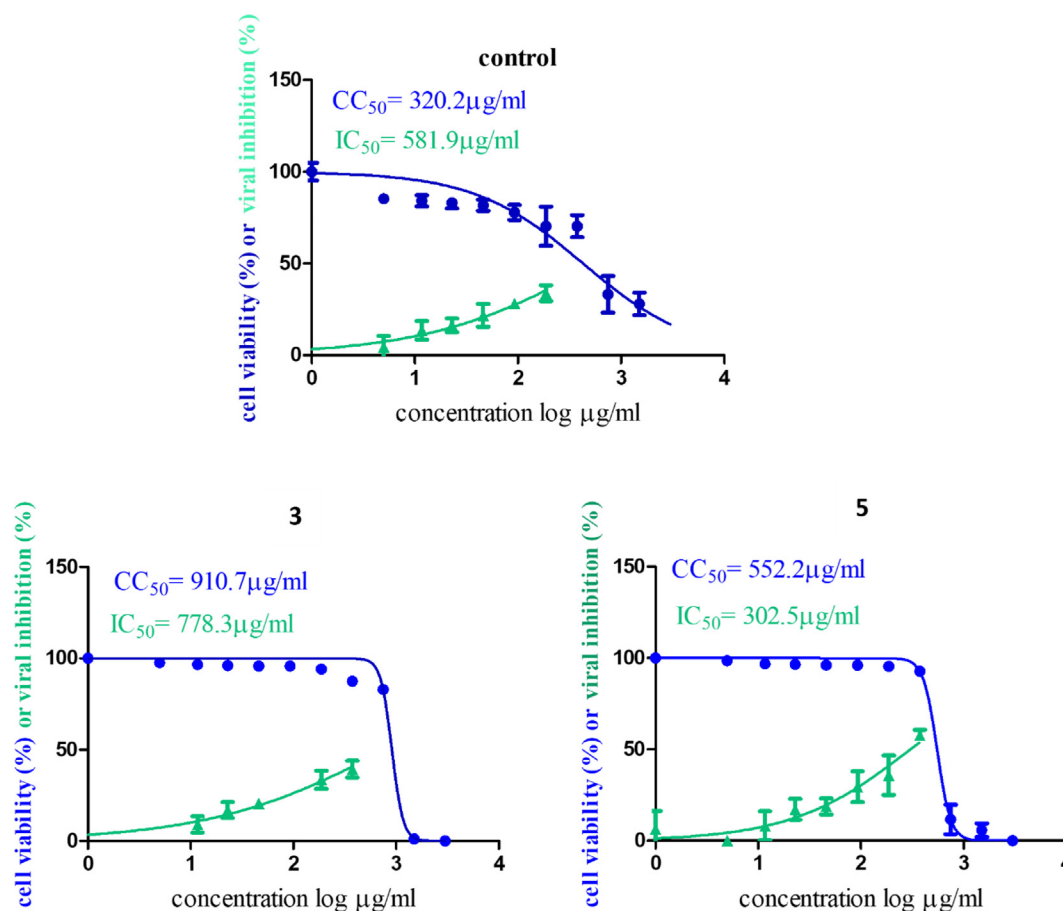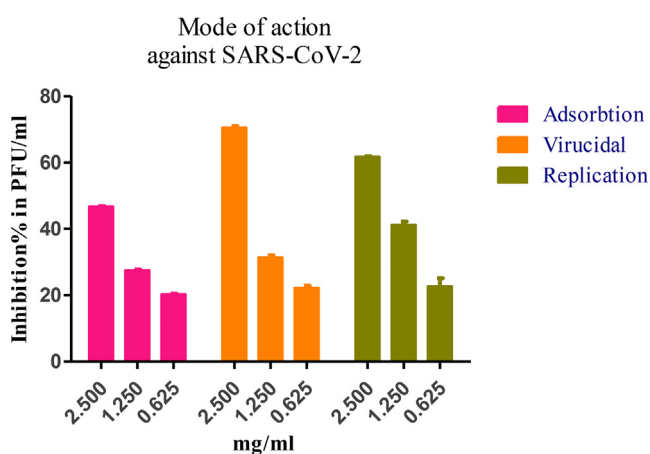

Fig. 3 Mode of action against SARS-CoV-2 for *C. zeylanicum* oil analysis by GraphPad Prism software (version 5.01) for concentrations against Inhibition % in plaque forming unit / mL (PFU/ML).

the range of 0.730. The mean droplet diameter was 280.2 nm, and a major portion of the NE was in the range of 9.357–3214 nm, as shown in Fig. 4. The two peaks at 297.3 and

3214 nm are related to agglomerated particles of *C. zeylanicum* oil. The *S. aromaticum* NE formulation showed an acceptable PDI in the range of 0.411. The mean droplet diameter was 185.3 nm, as shown in Fig. 5. It also showed 2 minor peaks with intensities of 6.3% and 1.2% showing sizes of 43.55 and 5505 nm, respectively. These peaks are mainly responsible for the PDI previously mentioned.

3.6.2. Zeta potential

Zeta potential values should be in the range of ± 30 mV to create an electrostatically stabilized NE (Baboota et al., 2007). The *C. zeylanicum* formulation zeta potential obtained was −10.3 mV as shown in Fig. 6 while the zeta potential of *S. aromaticum* NE was −21.7 mV as shown in Fig. 7, which indicates good stability.

As a result, there are limited chances of NE aggregating both during usage and in the biological environment. Steric repulsion is the cause of the emulsion's stabilization by non-ionic surfactants. The interface is negatively charged, according to zeta potential tests. By producing double-layer repulsion between the droplets, this charge will improve the stability of the emulsion. There is no correlation between stability and any zeta potential value. The composition of the oil, as well as the pH and electrolytes present in the water phase,
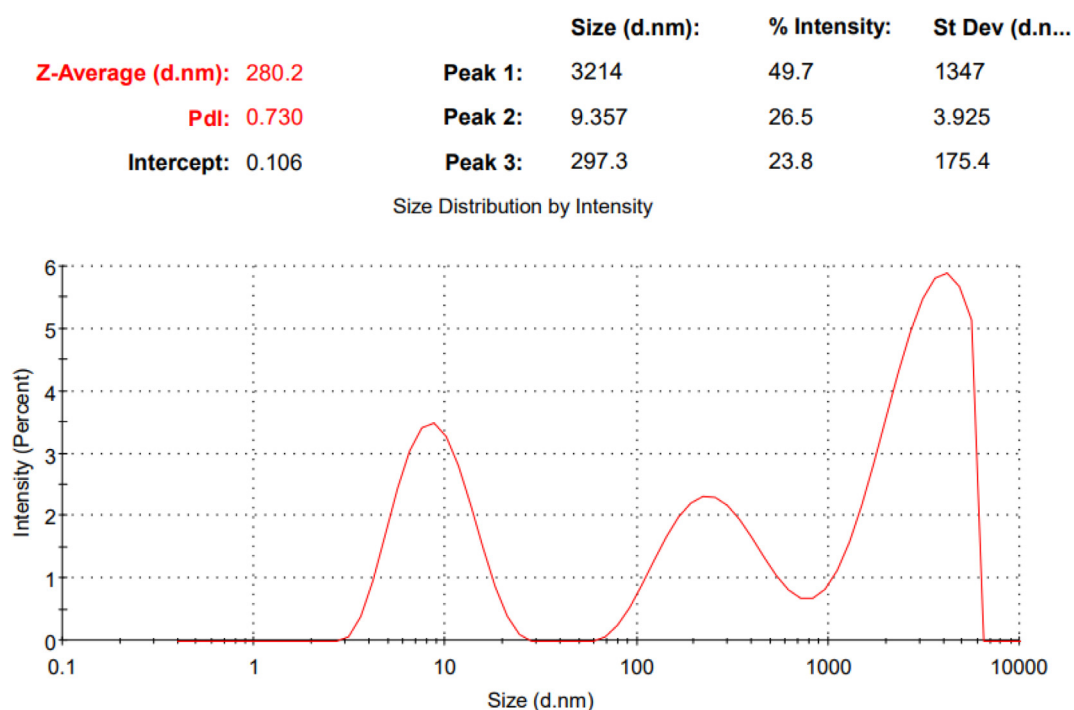
	Size (d.nm):	% Intensity:	St Dev (d.n...
Z-Average (d.nm): 280.2	**Peak 1:** 3214	49.7	1347
Pdl: 0.730	**Peak 2:** 9.357	26.5	3.925
Intercept: 0.106	**Peak 3:** 297.3	23.8	175.4

Size Distribution by Intensity

Fig. 4   The particle size & PDI of the prepared *C. zeylanicum* oil nano-emulsion.

	Size (d.nm):	% Intensity:	St Dev (d.n...
Z-Average (d.nm): 185.3	**Peak 1:** 210.7	92.5	73.24
Pdl: 0.411	**Peak 2:** 43.55	6.3	7.932
Intercept: 0.941	**Peak 3:** 5505	1.2	196.7
Result quality : Good			

Size Distribution by Intensity
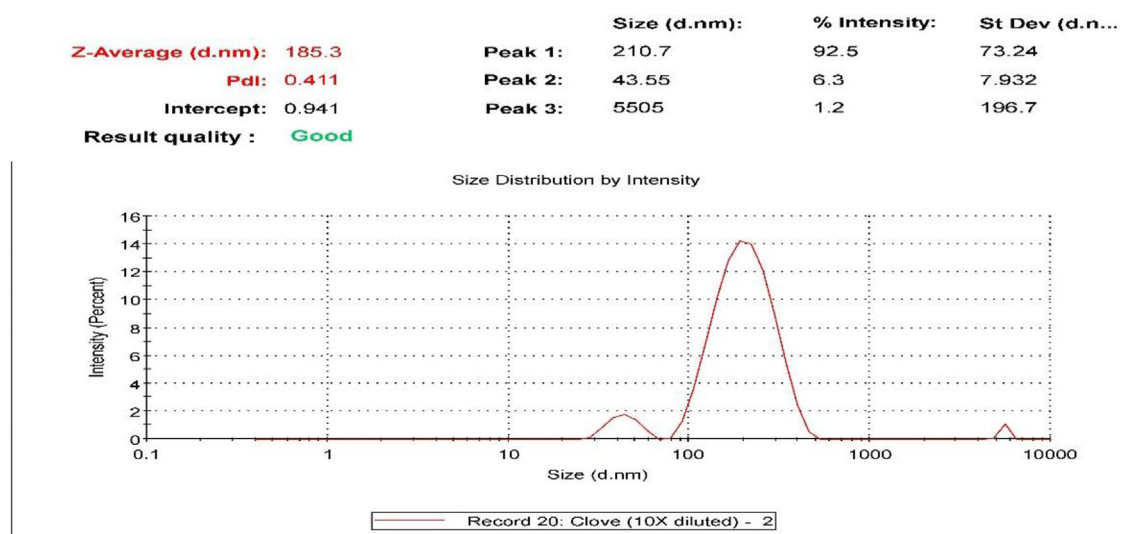
Record 20: Clove (10X diluted) – 2

Fig. 5   The particle size & PDI of the prepared *S. aromaticum* oil nano-emulsion.

all affect the origin of the contact charge (Binks and Whitby 2005).

3.6.3. Size and shape

1. Transmission electron microscopy characterization of *C. zeylanicum* oil NE showed shapeless, spherical, somewhat mono- or di-dispersed oil NE ranging in size from 53 to 85 nm, as shown in Fig. 8. While dynamic light scattering detected a size of 280 nm. This difference is due to the "hydrodynamic" nature of DLS approaches and their direct measurement of hydrodynamic parameters, often the translational and/or rotational diffusion coefficients, which are then theoretically connected to sizes and forms (Aly et al., 2019).

The morphological characterization of synthesized *S. aromaticum* NE gives the actual size and shape; the droplets in the NE appear dark and spherical in the range of 127–199 nm, as shown in Fig. 9. The droplet size was well correlated with the results obtained from droplet size analysis using dynamic light scattering, as the z-average showed was 185.3 nm.
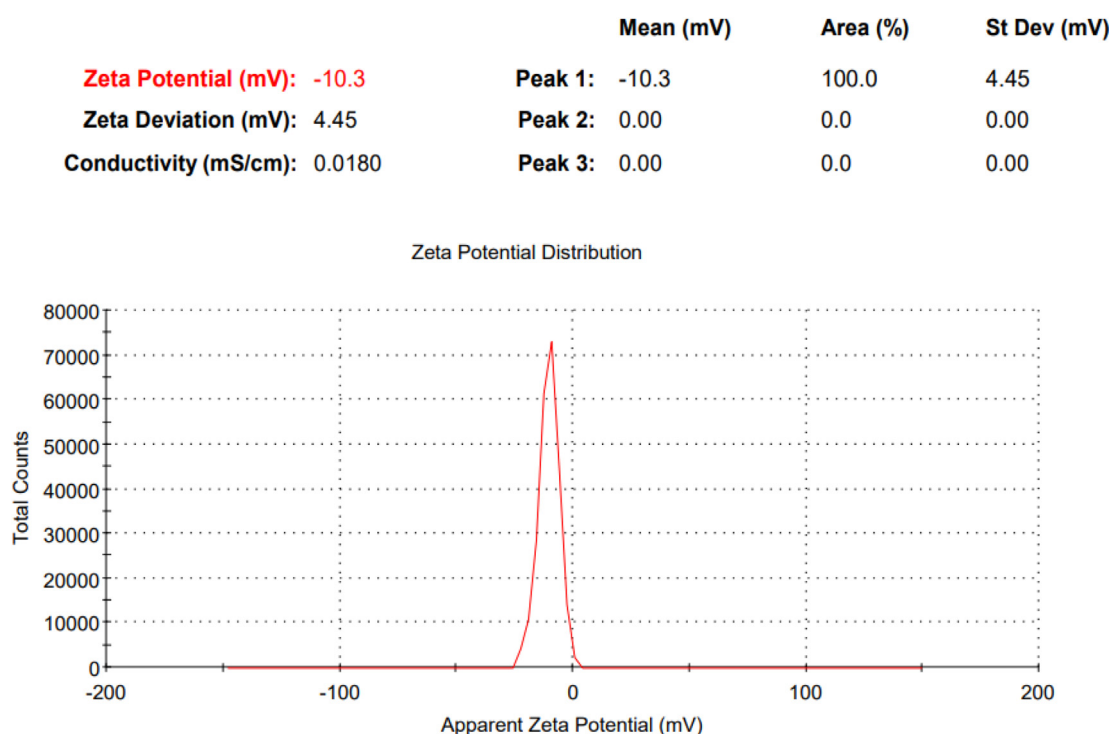
	Mean (mV)	Area (%)	St Dev (mV)
Zeta Potential (mV): -10.3	Peak 1: -10.3	100.0	4.45
Zeta Deviation (mV): 4.45	Peak 2: 0.00	0.0	0.00
Conductivity (mS/cm): 0.0180	Peak 3: 0.00	0.0	0.00

Zeta Potential Distribution

Fig. 6 The zeta potential of the prepared *C. zeylanicum* oil nano-emulsion.

	Mean (mV)	Area (%)	St Dev (mV)
Zeta Potential (mV): -21.7	Peak 1: -21.7	100.0	3.05
Zeta Deviation (mV): 3.05	Peak 2: 0.00	0.0	0.00
Conductivity (mS/cm): 0.0107	Peak 3: 0.00	0.0	0.00
Result quality : Good			

Zeta Potential Distribution
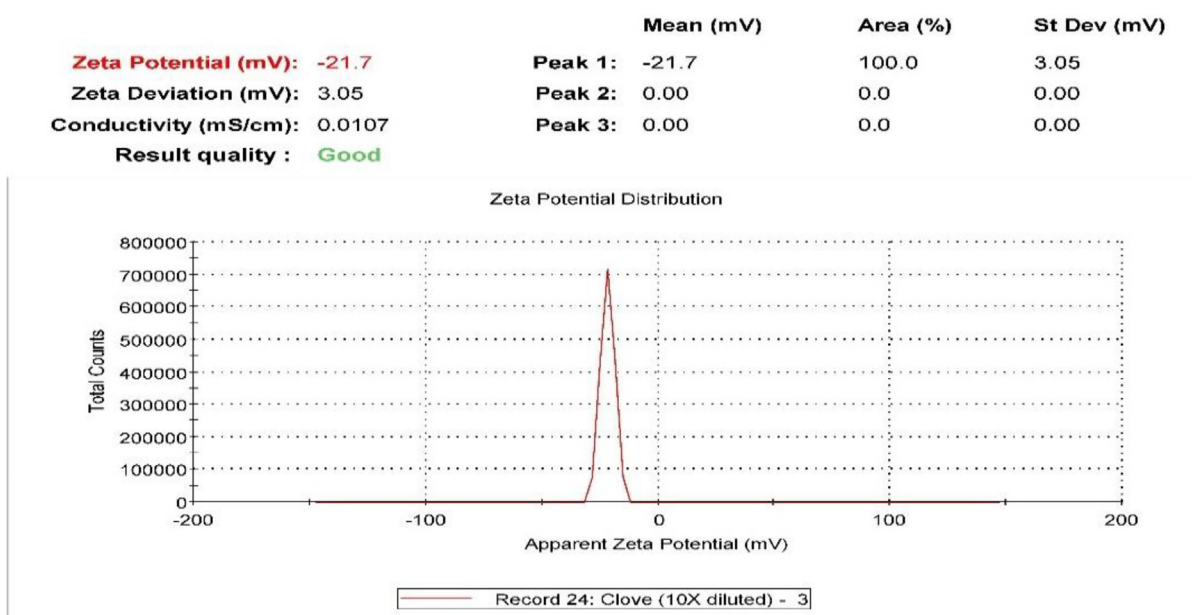

Record 24: Clove (10X diluted) - 3

Fig. 7 The zeta potential of the prepared *S. aromaticum* oil nano-emulsion.

3.7. GC–MS analysis of biologically active essential oils

After screening the distilled essential oils of *O. majorana, S. aromaticum, C. carvi, C. zeylanicum, L. nobilis, P. graveolens, F. vulgare, and E. globulus* as antimicrobial and antiviral agents, the potent active oil/or oils were selected for GC–MS analysis. The essential oils of *S. aromaticum* and *C. zeylanicum* exhibited the highest activities and were subjected to GC–MS

analysis to explore the constituents responsible for their potency.

The chromatograms representing the identified peaks of *S. aromaticum* and *C. zeylanicum* essential oils are presented in (Fig. S1 and S2), respectively. The identified compounds of both *S. aromaticum* and *C. zeylanicum* essential oils were presented in (Tables 3 and 4), respectively. Also, the chemical structures of the identified compounds in both essential oils are given in (Fig. 10).
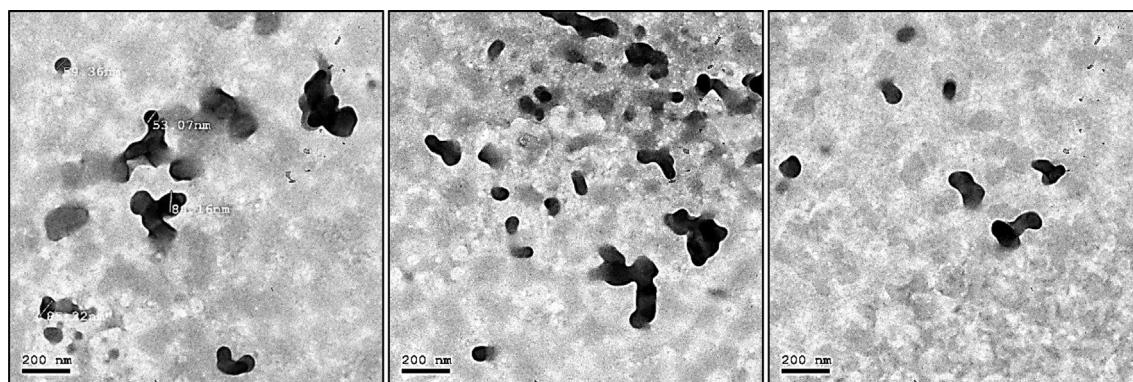
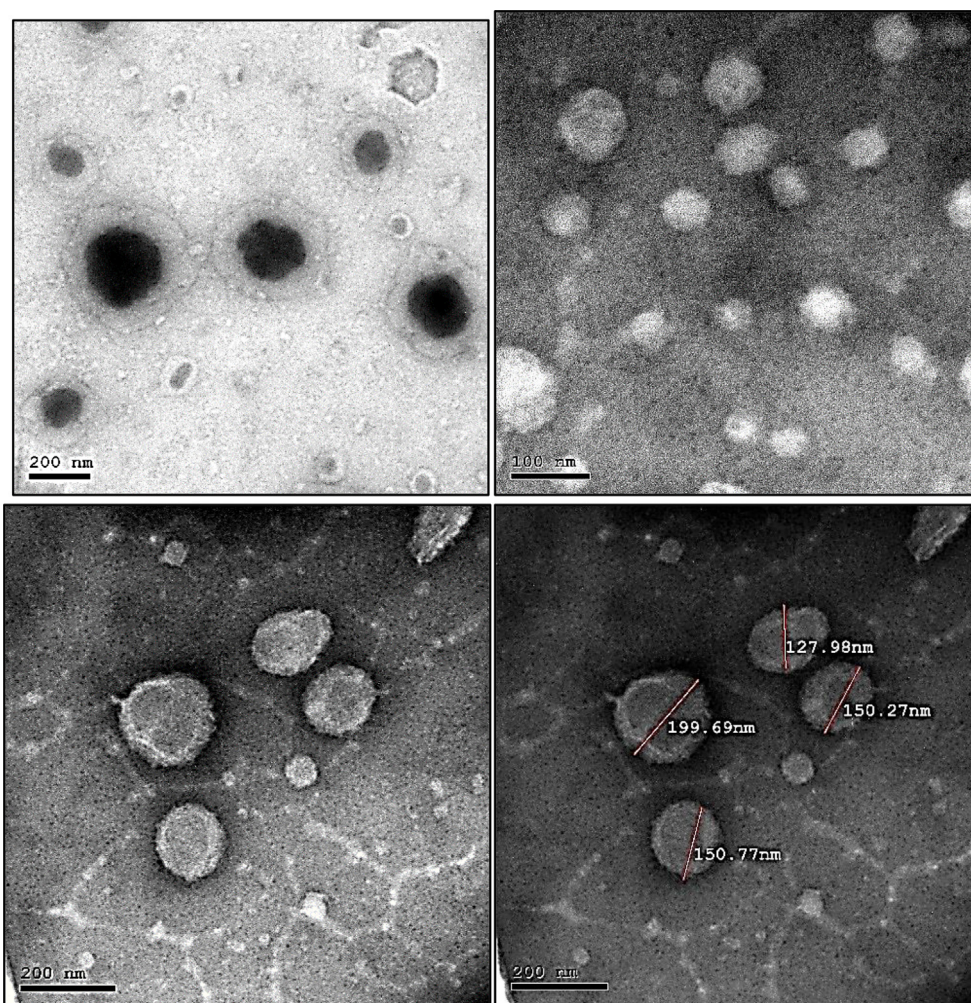**Fig. 8** The TEM images of the prepared *C. zeylanicum* oil nano-emulsion.

Fig. 9 The TEM images of the prepared *S. aromaticum* oil nano-emulsion.

4. Discussion

In this work, we examined the antibacterial activity of eight selected edible medicinal plants' essential oils against different Gram-positive and Gram-negative strains. The most efficient essential oils as antibacterial agents were those from *S. aromaticum* and *C. zeylanicum*. This was in accordance with the study published by (Anandhi et al., 2022) that claimed the presence of cinnamaldehyde, benzaldehyde, benzoic acid, and cinnamic acid in *C. zeylanicum* oil contributed to its effectiveness. Our study revealed that the essential oil of *C. zeylanicum* was more active against *S. aureus* than *E. coli*, which had MIC values of 1 and ≤ 0.5 μg/mL, respectively. This result was consistent with the research described by (Salma et al., 2020). According to the current investigation, *S. aromaticum* essential oil showed antibacterial activity against *S. aureus* and *E. coli*

Table 3 GC–MS analysis of *S. aromaticum* essential oil.

Peak No	R_t (min)	RelativeArea (%)	Mol. formula	Identified Compounds	Chemical Class
1	10.22	0.05	$C_{15}H_{24}$	α-Cubebene	Sesquiterpenes
2	10.82	0.19	$C_{15}H_{24}$	α-Copaene	Sesquiterpenes
3	12.65	14.65	$C_{15}H_{24}$	Caryophyllene	Sesquiterpenes
4	13.69	0.85	$C_{15}H_{24}$	Humulene	Sesquiterpenes
5	14.03	0.02	$C_{15}H_{24}$	Germacrene D	Sesquiterpenes
6	14.46	0.04	$C_{15}H_{24}$	*β*-Gurjunene	Sesquiterpenes
7	14.85	0.01	$C_8H_8O_3$	Methyl salicylate	organic compound
8	15.10	0.32	$C_{15}H_{24}$	*delta*-Cadinene	Sesquiterpenes
9	15.47	0.04	$C_{15}H_{24}$	Cubenene	Sesquiterpenes
10	16.14	0.02	$C_{15}H_{22}$	*trans*-calamenene	Sesquiterpenes
11	18.31	0.03	$C_{15}H_{26}$	Patchoulane	Sesquiterpenes
12	20.51	82.5	$C_{10}H_{12}O_2$	Eugenol	Phenylpropanoids
13	21.67	1.25	$C_{12}H_{14}O_3$	Eugenol Acetate	Phenylpropanoids
14	22.53	0.03	$C_9H_{10}O$	chavicol	Phenylpropene

Table 4 GC–MS analysis of *C. zeylanicum* essential oil.

Peak No	R_t (min)	Relative Area %	Mol. formula	Identified Compounds	Chemical Class
1	10.58	0.1	C_7H_6O	Benzaldehyde	aromatic aldehyde
2	10.80	0.27	$C_{15}H_{24}$	α-Copaene	Sesquiterpenes
3	12.41	0.05	$C_{10}H_{16}$	Santolinatriene	branched unsaturated hydrocarbons
4	13.65	0.01	$C_{15}H_{24}$	Humulene	Sesquiterpenes
5	13.99	0.13	$C_{15}H_{24}$	Germacrene D	Sesquiterpenes
6	14.42	0.02	$C_{15}H_{24}$	*β*-Gurjunene	Sesquiterpenes
7	14.61	0.16	$C_{15}H_{24}$	NI	——
8	14.91	0.12	$C_9H_{10}O$	3-Phenylpropanal	Phenylpropanoids
9	15.09	0.24	$C_{15}H_{24}$	*delta*-Cadinene	Sesquiterpenes
10	15.29	0.02	$C_{15}H_{22}$	α-Curcumene	aromatic monoterpenoids
11	15.45	0.03	$C_{15}H_{24}$	*β*-Curcumene	aromatic monoterpenoids
12	16.14	0.11	$C_{15}H_{22}$	*cis*-Calamenene	Sesquiterpenes
13	16.60	0.18	C_9H_8O	2-Propenal, 3-phenyl-	Phenylpropanoids
14	17.29	0.05	$C_{13}H_{16}$	3,4-Dihydrocadalene	Sesquiterpenes
15	18.86	97.5	C_9H_8O	*cis*-Cinnamic aldehyde	Phenylpropanoids
16	19.43	0.07	$C_{15}H_{24}$	NI	——
17	20.28	0.07	$C_{11}H_{12}O_2$	Cinnamyl acetate	Phenylpropanoids
18	20.41	0.02	$C_{12}H_{14}O_3$	Acetyleugenol	Phenylpropanoids
19	20.86	0.04	$C_{15}H_{24}$	γ-Muurolene	Sesquiterpenes
20	21.00	0.09	$C_{15}H_{24}$	α-Muurolene	Sesquiterpenes
21	21.17	0.08	$C_{15}H_{24}$	*β*-Copaene	Sesquiterpenes
22	21.47	0.02	$C_{15}H_{24}$	α-farnesene	Hydrocarbons
23	21.77	0.02	$C_{13}H_{16}O_2$	(E)-1-Hydroxy-1-phenyl-4-hepten-4-one	Benzene and substituted derivatives
24	21.87	0.01	$C_9H_{10}O$	2-Propen-1-ol, 3-phenyl-	Phenylpropanoids
25	23.28	0.01	$C_{14}H_{21}NO$	2-[(Benzylamino)methyl]-4-methyl-1-penten-3-ol	Benzene and substituted derivatives
26	23.72	0.46	$C_{10}H_{10}O_2$	2-Methoxycinnamaldehyde	Phenylpropanoids
27	29.96	0.11	$C_{10}H_{15}NO$	NI	——

NI = not identified.

with MIC values of 8 and 4 g/mL, respectively. These findings are consistent with those of (Pandey and Singh 2011), who reported that the MIC values of the methanolic extract of *S. aromaticum* against *S. aureus* and *E. coli* were 0.38 and 2.13 µg/mL, respectively. The antibacterial activity of the prepared NE formulation of the two potent antibacterial essential oils, *C. zeylanicum* and *S. aromaticum*, was investigated. Our work revealed that the formulated NE of *C. zeylanicum* essential oil enhanced the antibacterial activity by decreasing the MIC value by at least two folds, in which the MIC value of *C. zeylanicum* NE against *E. coli* and *K. pneumoniae* was decreased from 1 µg/ml for each to ≤ 0.5 for each. The results of the current investigation are in line with those published by (Valizadeh et al., 2018), who found that NE formulation
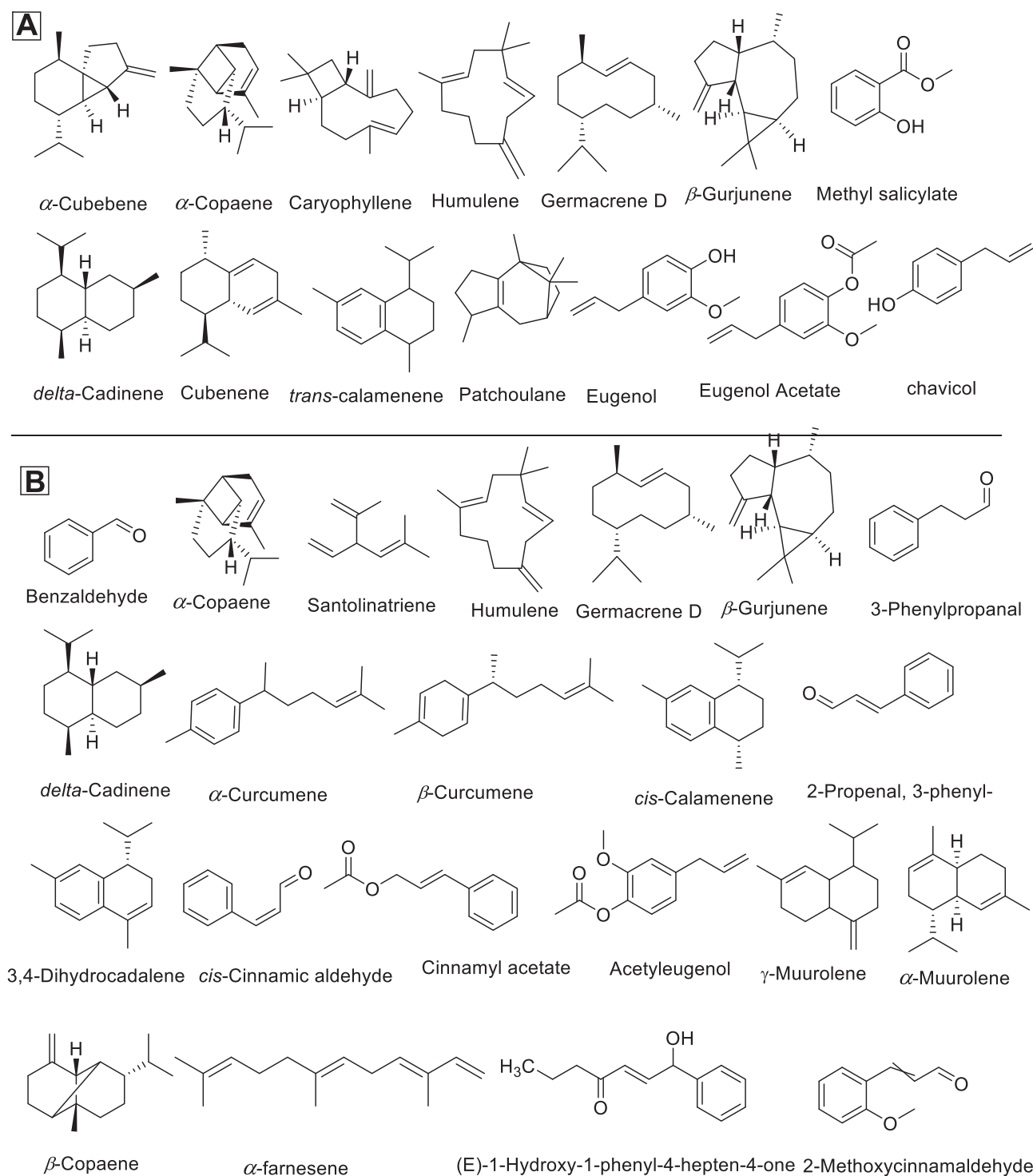
Fig. 10 Chemical structure of the identified compounds using GC–MS analysis; A: *Syzygium aromaticum* essential oil and B: *Cinnamomum zeylanicum* essential oil.

increased the antibacterial activity of *C. zeylanicum* while lowering the MIC values for *S. aureus* and *E. coli* by two-folds. Similarly, the NE of *S. aromaticum* essential oil was found to potentiate the antibacterial activity via the decrease of the MIC values against *E. coli and S. aureus* from 4 and 8 µg/mL respectively, to 2 µg/mL for each. This finding was consistent with the finding of (Anwer et al., 2014) who reported an

enhancement of the antibacterial activity of *S. aromaticum* in NE form. The previously mentioned study showed that the MIC of NE was observed in the range of 0.075–0.300 % w/w as compared to pure oil (MICs of 0.130–0.500 % w/w). Another work performed by Shahavi, *et al.* showed that *S. aromaticum* NE displayed antibacterial activity with MICs of 16 and 32 g/mL against *E. coli* and *Bacillus cereus*, respectively

(Shahavi et al., 2016). In contrast to the prominent antibacterial activity of *C. zeylanicum* and *S. aromaticum* essential oils, the current study reported elevated MIC values of *F. vulgare* essential oil against *S. aureus*, *E. coli*, and *P. aeruginosa*. This finding was related to a lesser extent to the findings of (Abdurahim et al., 2017), who reported the moderate antibacterial activity of *Foeniculum vulgare* essential oil and found that the MIC of the fennel seed EO ranged from 0.781 to 25 µl /mL. In addition to their antibacterial properties, EOs are also tested for their cytotoxicity, which is expressed in terms of CC_{50} (50% cytotoxic concentration), or the EO concentration that results in a 50% reduction in cell viability. This is done to make sure that the EOs are not toxic to host cells at the tested concentrations. The value of IC_{50} (50 % infection concentration), or the amount of EO needed to lower viral infection by 50%, is used to measure viral activity. The ratio of CC_{50} to IC_{50} is used to construct the antiviral selectivity index (SI), which serves as a gauge of EO's therapeutic appropriateness (Pilau et al., 2011). When defining the anti-infective potential of natural products, IC_{50} values should fall below a cutoff of 100 µg/mL for mixtures and 25 µM for pure compounds (Cos et al., 2006), and the acceptable SI values are those greater than 4 (Stránská et al., 2005). The results of cytotoxicity showed that the safest oil was *F. vulgare* oil followed by *L. nobilis*, *C. carvi*, *S. aromaticum* and *Eucalyptus globulus*.

The antiviral activity of *S. aromaticum* and *C. zeylanicum* essential oils was demonstrated against a variety of viral strains, including influenza A, parainfluenza virus, and HSV-1 viruses (Ovadia 2006). As a substitute for human norovirus, *S. aromaticum* demonstrated antiviral efficacy against feline calicivirus (Aboubakr et al., 2016). Furthermore, Potato virus-Y (PVY) was inhibited by *S. aromaticum* essential oil NE (Shafie 2017). Along with other plants including *C. zeylanicum*, ginger, black pepper, garlic, neem, and basil, clove are mentioned as one of the most often utilized spices and herbs during the present COVID-19 pandemic (Singh et al., 2021). Herbalists from Salé Prefecture in Morocco are also using *S. aromaticum* to treat and prevent COVID-19 (Chaachouay et al., 2021). Some computational research has suggested clove phytocompounds as effective anti-COVID-19 medications from a molecular perspective (Joshi et al., 2020). Numerous research teams looked at the primary component of cloves, eugenol, for its antiviral properties. Pure eugenol was utilized as the reference substance for anti-HSV in a study (Tragoolpua and Jatisatienr 2007), and it was discovered that it had greater antiviral activity than the ethanol extracts of whole clove buds. Benencia and Courreges (Benencia and Courrèges 2000), reported that eugenol inhibited the replication of HSV-1 and HSV-2 with IC_{50} values of 25.6 µg/mL and 16.2 µg/mL, respectively (Dai et al., 2013). The influenza A virus (IAV) was similarly susceptible, being able to withstand the antiviral effects of eugenol, which was able to stop IAV replication. Additionally, it was discovered to be effective *in vitro* as an Ebola virus inhibitor (Lane et al., 2019). According to a recent study, eugenol interacted with the SARS-CoV-2 spike (S1) protein and significantly inhibited the entry of pseudo-type SARS-CoV-2 into human ACE2-expressing HEK293 cells. Also, eugenol modified NF-kB, IL-6, IL-1β, and TNF-α in human A549 lung cells (Paidi et al., 2021). The antiviral activity of *C. zeylanicum* was also varied. In one study, commercial essential oils such as lavender, bergamot, lemongrass, and influenza type A (H_1N_1) were tested

for their *in vitro* antiviral activity. The oils underwent testing in both the liquid (0.3% concentration) and vapor phases. The liquid phase of H_1N_1 was totally suppressed by the oils of cinnamon, bergamot, thyme, and lemongrass. However, after 30 min of exposure, only cinnamon leaf essential oil showed 100% inhibition in the vapor phase. However, in the vapor phase, 100% inhibition was observed only for cinnamon leaf essential oil after 30 min of exposure (Vimalanathan and Hudson 2014). It also demonstrated dual efficacy, particularly against *S. aureus* and *S. pneumoniae*, suggesting that it might be useful in the treatment of influenza and post-influenza bacterial pneumonia infections. (Brochot et al., 2017). Furthermore, it had antiviral activity against H_7N_3 influenza A (Fatima et al., 2016). The main chemical component of *C. zeylanicum* oil is cinnamaldehyde. Several research teams looked at it for its antiviral properties. According to a study by (Liu et al., 2009) cinnamaldehyde inhibited the growth of adenovirus type 3 in a concentration-dependent manner with a virus inhibition rate of 3–58.6%. In addition, the cinnamaldehyde-treated group had lower levels of caspase-3, caspase-8, and caspase-9 protein expression than the virus control group did. In a different investigation, cinnamaldehyde suppressed influenza A/PR/8 virus development in a dose-dependent way (20 – 200 microM) and post-transcriptionally prevented the synthesis of viral proteins (Hayashi et al., 2007). In bronchoalveolar lavage fluid, cinnamaldehyde had the potential to decrease influenza A/PR/8 viral maturation (Hayashi et al., 2007). In a computational study, the S1 unit of the spike protein, which is in charge of binding to the angiotensin converting enzyme 2 (ACE2), was examined to determine the inhibitory effects of various major constituents from essential oils (star anise, cinnamon, tea tree, lavender, thyme, mint, etc). (ACE2). The findings demonstrated that additional chemicals, including cinnamaldehyde and cinnamyl acetate, hindered viral replication in the host cells (Damiescu et al., 2022). Additionally, characteristics related to the virus, such as the viral load kinetics and viral protein structure, affect the reported antiviral activity of EOs. The direct contact of the EO with the virus is the most frequent action mechanism; however, the entire mechanism is still not fully understood (Ralambondrainy et al., 2018, Ma and Yao 2020).

The COVID-19 pandemic is still a serious and widespread health issue in the world today. From ancient times, essential oils have been known to have a wide range of bioactivity, including antimicrobials and antivirals. Several studies have shown that essential oils may have antiviral properties against a variety of viruses, including HSV-1, adenoviruses, ECHO-9, Coxsackie B1, and H_1N_1 (Sinico et al., 2005, Loizzo et al., 2008, Brochot et al., 2017, Abou Baker et al., 2021). At present, computer-aided docking and few *in vitro* studies are available for the antiviral effects of essential oils against the SARS-CoV-2 (Senthil Kumar et al., 2020, Lionis et al., 2021, Ćavar Zeljković et al., 2022, Esharkawy et al., 2022). In the current work, the most potent antiviral essential oils tested against SARS-CoV-2 virus were *C. zeylanicum* followed by *S. aromaticum*. This antiviral activity was in accordance with the previous studies reported as follows: according to an *in-silico* study published by (Kulkarni et al., 2020), cinnamaldehyde and cinnamyl acetate have shown superior ability to inhibit the S1 subunit of the S proteins of SARS-Cov-2, and cinnamaldehyde was the top-scoring molecule out of the thirteen compounds that were evaluated. Another study used molecu-

lar docking techniques to test the effectiveness of 171 essential oil components against various SARC-CoV-2 proteins, including the main viral proteases (Mpro), ADP-ribose-1-phosphatases (SARS-CoV-2 ADRP), endoribonucleases (SARS-CoV-2 Nsp15/NendoU), and human angiotensin-converting enzyme (hACE spike proteins (SARS-CoV-2 rS). Of the 171 compounds that were evaluated, (E,E)-farnesene (one of the *C. zeylanicum* EO's components) showed stronger affinity with SARS-CoV-2 Mpro, indicating that this compound or its essential oil can limit viral replication (Da Silva et al., 2020). Silva and colleagues used molecular docking techniques to screen the anti-SARC-CoV-2 efcacies of eugenol, menthol, and carvacrol, major components of EOs, against various proteins targets of SARS-CoV-2. The docking score of eugenol (main component of the *S. aromaticum* EO) against various proteins targets of SARS-CoV-2, revealed that this compound has binding afnities towards SARS-CoV-2 spike protein, main protease (Mpro), RNA dependent RNA polymerase and human ACE-2 proteins, respectively (Da Silva et al., 2020). Even though the mechanism of action of these oils and their components was shown to be primarily through suppression of viral replication, essential oils and their key components have demonstrated strong antiviral efficacy to other coronaviruses, such as SARSCoV-1 (Senthil Kumar et al., 2020). After evaluation of the two potent essential oils, *C. zeylanicum* and *S. aromaticum,* as antiviral agents against SARS-CoV-2, the nano-emulsion formulation of the two previous oils were investigated. The results showed that the non-nanoemulsion form of the oil was found to be more active against the virus than the nano form, with an IC_{50} of 778.3 g/mL for *S. aromaticum* oil NE form and 302.5 g/mL for *C. zeylanicum* oil NE form. This indicates that the activity of these essential oil can be obtained through using them in pure form.

The primary mechanism of action of EOs is the suppression of viral attachment and entry because of their lipophilic properties, which enable them to interact with the lipid bilayer within the viral envelope. As further evidence that *S. aromaticum*'s effects on protease enzymes affect the replication step in the viral life cycle, methanol extracts of *S. aromaticum* demonstrated a strong *in vitro* activity of the extract in inhibiting the HCV protease, with a 90% protease inhibition at a concentration of 100 g/mL (Vicidomini et al., 2021). As a result, the cytoplasmic membrane's fluidity and permeability were changed, and at higher concentrations, the membranes were torn (Ma and Yao 2020). The mode of action for *C. zeylanicum* essential oil in this work was virucidal effect, which means that this oil affected the spike protein of the virus and reduced the virus's ability to cause infection. Moreover, the polymerase enzyme necessary for the viral propagation cycle was impacted by *C. zeylanicum* essential oil, which had an impact on replication. Our investigation determined that the interpretation of this activity was related to the influence of these oils on virus replication and virucidal impact.

The chemical characterization of the two potent essential oils, *S. aromaticum* and *C. zeylanicum*, as anti-bacterial and anti-SARS-CoV-2 agents was resolved by GC–MS analysis, which revealed fourteen and twenty-seven components, respectively. The oil constituents were identified by comparing their retention time and peak area with those from the Willey spectral library and from the literature. The main component of *S. aromaticum* oil was found to be eugenol (82.5%), followed by

caryophyllene (14.65%) and eugenol acetate (1.25%). Theis is in accord with those described in prior research, which all note that eugenol is the primary component of *S. aromaticum* essential oil, though there are some differences in its concentration (Jirovetz et al., 2006, Guan et al., 2007, Devi et al., 2010, Sulistyoningrum et al., 2017). On the other hand, cinnamaldehyde (97.69%) was the main ingredient in *C. zeylanicum* volatile oil along with several other minor constituents such as 2-Methoxy-cinnamaldehyde (0.46%), delta-cadinene (0.24%), and germacrene D (0.13%). According to the reported literature, the main components in *C. zeylanicum* essential oils are cinnamaldehyde, methoxy-cinnamaldehyde, cadinene, germacrene D, and cinnamyl alcohol, which agree with those identified in this study (Wang et al., 2009). It is well known that there are considerable differences in the consistency of distilled essential oil, which can be likened to a variety of agro-climatic factors (geographic, climatic, seasonal), plant maturity stages, plant metabolism adaptation, distillation conditions, and the plant part analyzed, among other things. (Anwar et al., 2009, Elgendy et al., 2017).

5. Conclusion

Essential oils from *C. zeylanicum* and *S. aromaticum* showed promising antibacterial and anti-SARS-CoV-2 properties. The mechanism by which *C. zeylanicum* oil exerts its antiviral activity may involve both the virucidal effect and its impact on viral reproduction. Additionally, the non-nanoemulsion form outperformed the nano-emulsion form in terms of selectivity index, making it easier for pharmaceutical industries to use essential oils without using nano-formulation. To ascertain the antiviral activity of these oils and/or their constituents and to clarify their potential modes of action, more *in vivo* investigations are required. Our results can be used to guide the creation of innovative formulations against COVID-19 for various food, pharmaceutical, cosmetic, and medical uses, as well as to support future *in vitro* and *in vivo* research to identify effective EOs. This work opens the gate to further investigations for preclinical and clinical studies of a wide range of edible EOs to alleviate certain respiratory tract infections.

Declaration of Competing Interest

The authors declare that they have no known competing financial interests or personal relationships that could have appeared to influence the work reported in this paper.

Appendix A. Supplementary material

Supplementary data to this article can be found online at https://doi.org/10.1016/j.arabjc.2023.104813.

References

Abdelhady, A. S., Y. A. ElShaier, M. S. Refaey, et al., 2022. Intelligent Drug Descriptors Analysis: Toward COVID-19 Drug Repurposing. Medical Informatics and Bioimaging Using Artificial Intelligence: Challenges, Issues, Innovations and Recent Developments. 173-191

Abdurahim, S. A., B. K. Elamin, A. A. Bashir, et al., 2017. In Vitro Test Of Antimicrobial Activity of Foeniculum Vulgare Mill. (Fennel) Essential Oil. 3, 1609-1614

Abou Baker, D.H., Amarowicz, R., Kandeil, A., et al, 2021. Antiviral activity of Lavandula angustifolia L. and Salvia officinalis L. essential oils against avian influenza H5N1 virus. J. Agric. Food Res. 4, 100135.

Aboubakr, H.A., Nauertz, A., Luong, N.T., et al, 2016. In vitro antiviral activity of clove and ginger aqueous extracts against Feline Calicivirus, a surrogate for human Norovirus. J. Food Prot. 79, 1001–1012.

Ács, K., Balázs, V.L., Kocsis, B., et al, 2018. Antibacterial activity evaluation of selected essential oils in liquid and vapor phase on respiratory tract pathogens. BMC Complement. Altern. Med. 18, 227.

Aly, U.F., Abou-Taleb, H.A., Abdellatif, A.A., et al, 2019. Formulation and evaluation of simvastatin polymeric nanoparticles loaded in hydrogel for optimum wound healing purpose. Drug Des. Devel. Ther. 13, 1567.

Anandhi, P., M. Tharani, S. Rajeshkumar, et al., 2022. Antibacterial activity of cinnamon and clove oil against wound pathogens. J Popul Ther Clin Pharmacol. 28, e41-e46.

Anwar, F., M. A. Ali, A. I. Hussain, et al., 2009. Antioxidant and antimicrobial activities of essential oil and extracts of fennel (Foeniculum vulgare Mill.) seeds from Pakistan. 24, 167-170

Anwer, M.K., Jamil, S., Ibnouf, E.O., et al, 2014. Enhanced antibacterial effects of clove essential oil by nanoemulsion. J. Oleo Sci. 63, 347–354.

Baboota, S., Shakeel, F., Ahuja, A., et al, 2007. Design, development and evaluation of novel nanoemulsion formulations for transdermal potential of celecoxib. Acta Pharm. 57, 315–332.

Balázs, V.L., Horváth, B., Kerekes, E., et al, 2019. Anti-Haemophilus activity of selected essential oils detected by TLC-direct bioautography and biofilm inhibition. Molecules 24, 3301.

Benencia, F., Courrèges, M.C., 2000. In vitro and in vivo activity of eugenol on human herpesvirus. Phytother. Res. 14, 495–500.

Binks, B.P., Whitby, C.P., 2005. Nanoparticle silica-stabilised oil-in-water emulsions: improving emulsion stability. Colloids Surf. A Physicochem. Eng. Asp. 253, 105–115.

Brochot, A., Guilbot, A., Haddioui, L., et al, 2017. Antibacterial, antifungal, and antiviral effects of three essential oil blends. Microbiologyopen 6, e00459.

Campolo, O., Giunti, G., Laigle, M., et al, 2020. Essential oil-based nano-emulsions: Effect of different surfactants, sonication and plant species on physicochemical characteristics. Ind. Crop. Prod. 157, 112935.

Ćavar Zeljković, S., E. Schadich, P. Džubák, et al., 2022. Antiviral activity of selected lamiaceae essential oils and their monoterpenes against SARS-Cov-2. Frontiers in Pharmacology. 1589.

Chaachouay, N., Douira, A., Zidane, L., 2021. COVID-19, prevention and treatment with herbal medicine in the herbal markets of Salé Prefecture, North-Western Morocco. Eur. J. Integr. Med. 42, 101285.

Cos, P., Vlietinck, A.J., Berghe, D.V., et al, 2006. Anti-infective potential of natural products: how to develop a stronger in vitro 'proof-of-concept'. J. Ethnopharmacol. 106, 290–302.

Da Silva, J.K.R., Figueiredo, P.L.B., Byler, K.G., et al, 2020. Essential oils as antiviral agents, potential of essential oils to treat SARS-CoV-2 infection: an in-silico investigation. Int. J. Mol. Sci. 21, 3426.

Dai, J.-P., Zhao, X.-F., Zeng, J., et al, 2013. Drug screening for autophagy inhibitors based on the dissociation of Beclin1-Bcl2 complex using BiFC technique and mechanism of Eugenol on anti-influenza A virus activity. PLoS One 8, e61026.

Damiescu, R., Lee, D.Y.W., Efferth, T., 2022. Can essential oils provide an alternative adjuvant therapy for COVID-19 infections and pain management at the same time? Pharmaceuticals (Basel) 15, 1387.

Denizot, F., Lang, R., 1986. Rapid colorimetric assay for cell growth and survival. modifications to the tetrazolium dye procedure giving improved sensitivity and reliability. J. Immunol. Methods 89, 271–277.

Devi, K.P., Nisha, S.A., Sakthivel, R., et al, 2010. Eugenol (an essential oil of clove) acts as an antibacterial agent against Salmonella typhi by disrupting the cellular membrane. J. Ethnopharmacol. 130, 107–115.

Elgendy, E. M., H. S. Ibrahim, H. F. Elmeherry, et al., 2017. Chemical and Biological Comparative in Vitro Studies of Cinnamon Bark and Lemon Peel Essential Oils. 08, 110-125

El-Kased, R.F., 2016. Natural antibacterial remedy for respiratory tract infections. Asian Pac. J. Trop. Biomed. 6, 270–274.

Esharkawy, E.R., Almalki, F., Hadda, T.B., 2022. In vitro potential antiviral SARS-CoV-19-activity of natural product thymohydroquinone and dithymoquinone from Nigella sativa. Bioorg. Chem. 120, 105587.

Fatima, M., Zaidi, N.U., Amraiz, D., et al, 2016. In vitro antiviral activity of Cinnamomum cassia and its nanoparticles against H7N3 influenza A virus. J. Microbiol. Biotechnol. 26, 151–159.

Ghanbari, M., Salavati-Niasari, M., Mohandes, F., et al, 2022. Modified silicon carbide NPs reinforced nanocomposite hydrogels based on alginate-gelatin by with high mechanical properties for tissue engineering. Arab. J. Chem. 15, 103520.

Ghasemi, M., Turnbull, T., Sebastian, S., et al, 2021. The MTT assay: utility, limitations, pitfalls, and interpretation in bulk and single-cell analysis. Int. J. Mol. Sci. 22, 12827.

Guan, W., Li, S., Yan, R., et al, 2007. Comparison of essential oils of clove buds extracted with supercritical carbon dioxide and other three traditional extraction methods. Food Chem. 101, 1558–1564.

Hayashi, K., Imanishi, N., Kashiwayama, Y., et al, 2007. Inhibitory effect of cinnamaldehyde, derived from Cinnamomi cortex, on the growth of influenza A/PR/8 virus in vitro and in vivo. Antiviral Res. 74, 1–8.

Horváth, G., Ács, K., 2015. Essential oils in the treatment of respiratory tract diseases highlighting their role in bacterial infections and their anti-inflammatory action: a review. Flavour Fragr. J. 30, 331–341.

Jirovetz, L., Buchbauer, G., Stoilova, I., et al, 2006. Chemical composition and antioxidant properties of clove leaf essential oil. J. Agric. Food Chem. 54, 6303–6307.

Joshi, T., Joshi, T., Sharma, P., et al, 2020. In silico screening of natural compounds against COVID-19 by targeting Mpro and ACE2 using molecular docking. Eur. Rev. Med. Pharmacol. Sci. 24, 4529–4536.

June, W. H. O. J. A., 2015. The top ten causes of death (http://www.who. int/mediacentre /factsheets/fs310/en/).

Karami, M., Ghanbari, M., Alshamsi, H.A., et al, 2021. Facile fabrication of Tl 4 HgI 6 nanostructures as novel antibacterial and antibiofilm agents and photocatalysts in the degradation of organic pollutants. Inorg. Chem. Front. 8, 2442–2460.

Kulkarni, S.A., Nagarajan, S.K., Ramesh, V., et al, 2020. Computational evaluation of major components from plant essential oils as potent inhibitors of SARS-CoV-2 spike protein. J. Mol. Struct. 1221, 128823.

Kuo, Y.C., Lin, L.C., Tsai, W.J., et al, 2002. Samarangenin B from Limonium sinense suppresses herpes simplex virus type 1 replication in Vero cells by regulation of viral macromolecular synthesis. Antimicrob. Agents Chemother. 46, 2854–2864.

Lane, T., Anantpadma, M., Freundlich, J.S., et al, 2019. The natural product Eugenol is an inhibitor of the Ebola virus in vitro. Pharm. Res. 36, 104.

Lionis, C., Karakasiliotis, I., Petelos, E., et al, 2021. A mixture of essential oils from three Cretan Aromatic Plants (thyme, Greek sage and Cretan dittany, CAPeo) inhibits SASR-CoV-2 proliferation: in vitro evidence and a Proof-of-Concept intervention study in mild ambulatory COVID-19-positive patients. MedRxiv 2021, 20248947.

Liu, L., Wei, F.-X., Qu, Z.-Y., et al, 2009. The antiadenovirus activities of cinnamaldehyde in vitro. Lab. Med. 40, 669–674.

Loizzo, M.R., Saab, A.M., Tundis, R., et al, 2008. Phytochemical analysis and in vitro antiviral activities of the essential oils of seven Lebanon species. Chem. Biodivers. 5, 461–470.

Ma, L., Yao, L., 2020. Antiviral effects of plant-derived essential oils and their components: an updated review. Molecules 25, 2627.

Molinari, G. J. P. B., 2009. Natural products in drug discovery: present status and perspectives. 13-27.

Nguyen-Ho, L., Nguyen-Nhu, V., Tran-Thi, T.-T., et al, 2022. Severe chronic cough relating to post-COVID-19 interstitial lung disease: a case report. Asia Pac. Allergy 12, e42.

Oriola, A.O., Oyedeji, A.O., 2022. Plant-derived natural products as lead agents against common respiratory diseases. Journal 27, 3054.

Ovadia, M., 2006. Antiviral preparations obtained from a natural cinnamon extract.

Paidi, R.K., Jana, M., Raha, S., et al, 2021. Eugenol, a component of Holy Basil (Tulsi) and common spice clove, inhibits the interaction between SARS-CoV-2 Spike S1 and ACE2 to induce therapeutic responses. J. Neuroimmun. Pharmacol. 16, 743–755.

Pandey, A., Singh, P., 2011. Antibacterial activity of Syzygium aromaticum (clove) with metal ion effect against food borne pathogens. Asian J. Plant Sci. Res. 1, 69–80.

Paudel, S.K., Bhargava, K., Kotturi, H., 2019. Antimicrobial activity of cinnamon oil nanoemulsion against Listeria monocytogenes and Salmonella spp. on melons. LWT 111, 682–687.

Pilau, M.R., Alves, S.H., Weiblen, R., et al, 2011. Antiviral activity of the Lippia graveolens (Mexican oregano) essential oil and its main compound carvacrol against human and animal viruses. Braz. J. Microbiol. 42, 1616–1624.

Ralambondrainy, M., Belarbi, E., Viranaicken, W., et al, 2018. In vitro comparison of three common essential oils mosquito repellents as inhibitors of the Ross River virus. PLoS One 13, e0196757.

Refaey, M.S., Abouelela, M.E., El-Shoura, E.A., et al, 2022. In vitro anti-Inflammatory activity of Cotula anthemoides essential oil and in silico molecular docking of its bioactives. Molecules 27, 1994.

Salma, U., Sultana, S., Saha, S.K., et al, 2020. In vitro antibacterial activity of ethanol extracts of Cinnamomum zeylanicum against Pseudomonas aeruginosa. Mymensingh Med. J. 29, 248–253.

Schuhmacher, A. E., J. r. Reichling and P. Schnitzler, 2003. Virucidal effect of peppermint oil on the enveloped viruses herpes simplex virus type 1 and type 2 in vitro. Phytomedicine : international journal of phytotherapy and phytopharmacology. 10, 504-510.

Schwalbe, R., Steele-Moore, L., Goodwin, A.C., 2007. Antimicrobial Susceptibility Testing Protocols. CRC Press.

Senthil Kumar, K., Gokila Vani, M., Wang, C.-S., et al, 2020. Geranium and lemon essential oils and their active compounds downregulate angiotensin-converting enzyme 2 (ACE2), a SARS-CoV-2 spike receptor-binding domain, in epithelial cells. Plants 9, 770.

Shafie, R.M., 2017. Antiviral activity of clove oil nanoemulsion against potato virus-Y (PVY). Egypt. J. Phytopathol. 45, 15–31.

Shahavi, M.H., Hosseini, M., Jahanshahi, M., et al, 2016. Clove oil nanoemulsion as an effective antibacterial agent: Taguchi optimization method. Desalin. Water Treat. 57, 18379–18390.

Shahavi, M.H., Hosseini, M., Jahanshahi, M., et al, 2019. Evaluation of critical parameters for preparation of stable clove oil nanoemulsion. Arab. J. Chem. 12, 3225–3230.

Silva, J.R.A., Kruger, H.G., Molfetta, F.A., 2021. Drug repurposing and computational modeling for discovery of inhibitors of the main protease (M pro) of SARS-CoV-2. RSC Adv. 11, 23450–23458.

Singh, N. A., P. Kumar, Jyoti, et al., 2021. Spices and herbs: Potential antiviral preventives and immunity boosters during COVID-19. Phytother Res. 35, 2745-2757.

Sinico, C., De Logu, A., Lai, F., et al, 2005. Liposomal incorporation of Artemisia arborescens L. essential oil and in vitro antiviral activity. Eur. J. Pharm. Biopharm. 59, 161–168.

Stránská, R., Schuurman, R., Nienhuis, E., et al, 2005. Survey of acyclovir-resistant herpes simplex virus in the Netherlands: prevalence and characterization. J. Clin. Virol. 32, 7–18.

Sulistyoningrum, A. S., E. Saepudin, A. H. Cahyana, et al., 2017. Chemical profiling of clove bud oil (Syzygium aromaticum) from Toli-Toli and Bali by GC-MS analysis. 1862, 030089.

Tadros, T., Izquierdo, P., Esquena, J., et al, 2004. Formation and stability of nano-emulsions. Adv. Colloid Interface Sci. 108, 303–318.

Tragoolpua, Y., Jatisatienr, A., 2007. Anti-herpes simplex virus activities of Eugenia caryophyllus (Spreng.) Bullock & S. G. Harrison and essential oil, eugenol. Phytother. Res. 21, 1153–1158.

Unoh, Y., Uehara, S., Nakahara, K., et al, 2022. Discovery of S-217622, a noncovalent oral SARS-CoV-2 3CL protease inhibitor clinical candidate for treating COVID-19. J. Med. Chem. 65, 6499–6512.

Valizadeh, A., M. Shirzad, F. Esmaeili, et al., 2018. Increased antibacterial activity of Cinnamon Oil Microemulsionin Comparison with Cinnamon Oil Bulk and Nanoemulsion.

Vicidomini, C., V. Roviello and G. N. Roviello, 2021. Molecular basis of the therapeutical potential of clove (Syzygium aromaticum L.) and clues to its anti-COVID-19 utility. Molecules. 26, 1880.

Vandepitte, J., Verhaegen, J., Engbaek, K., et al, 2003. Basic laboratory procedures in clinical bacteriology. World Health Organization.

Vimalanathan, S., Hudson, J.B., 2014. Anti-influenza virus activity of essential oils and vapors. Am. J. Essent. Oils Nat. Prod. 2, 47–53.

Wang, R., Wang, R., Yang, B., 2009. Extraction of essential oils from five cinnamon leaves and identification of their volatile compound compositions. Innov. Food Sci. Emerg. Technol. 10, 289–292.

Wikler, M.A., 2006. Methods for dilution antimicrobial susceptibility tests for bacteria that grow aerobically: approved standard. Clsi (Nccls) 26, M7–M.

Zaidman, D., Gehrtz, P., Filep, M., et al, 2021. An automatic pipeline for the design of irreversible derivatives identifies a potent SARS-CoV-2 Mpro inhibitor. Cell Chem. Biol. 28 (1795–1806), e1795.

Zhang, L., Lin, D., Sun, X., et al, 2020. Crystal structure of SARS-CoV-2 main protease provides a basis for design of improved α-ketoamide inhibitors. Science 368, 409–412.

Zhu, W., Xu, M., Chen, C.Z., et al, 2020. Identification of SARS-CoV-2 3CL protease inhibitors by a quantitative high-throughput screening. ACS Pharmacol. Transl. Sci. 3, 1008–1016.